Surface Compression With Hierarchical Powell–Sabin B-Splines

Jan Maes Adhemar Bultheel

May 2004

Abstract

We show how to construct a stable hierarchical basis for piecewise quadratic C^1 continuous splines defined on Powell–Sabin triangulations. We prove that this hierarchical basis is well suited for compressing surfaces. Our compression method does not require the construction of wavelets which are usually expensive to compute, but instead we construct a stable quasi-interpolation scheme for our spline space which achieves optimal approximation order. Numerical experiments demonstrate the high compression rate of the algorithm.

1 Introduction

In this paper we look for a compression algorithm for the space $S_2^1(\Delta_{PS})$ of piecewise quadratic C^1 continuous splines on Powell–Sabin (PS) triangulations which does not require the construction of wavelets. Instead we use a hierarchical basis. Hereto we were inspired by the work of Hong and Schumaker [5] who have constructed a surface compression algorithm for the space of C^1 cubic splines defined on triangulations obtained from convex quadrangulations. Although stable wavelets for the space $S_2^1(\Delta_{PS})$ have been constructed in [11] we prefer not to use these wavelets for surface compression because of their substantial amount of computation time. The method presented here using hierarchical bases is easy to implement and is computationally efficient. We do not need to solve any systems of equations in either the decomposition or reconstruction phases.

Let Ω be a bounded polygonal domain in $\mathbb{R}^2$. The key to our compression method is the construction of a linear quasi-interpolation operator Q which maps $C(\Omega)$ onto the spline space $S_2^1(\Delta_{PS})$ in such a way that if f lies in a Sobolev space $W_p^{k+1}(\Omega)$ with $1 \leq k \leq 2$ and $2 \leq p \leq \infty$, then Qf approximates f and its derivatives to optimal order,

$$\|D_x^\alpha D_y^\beta (f - Qf)\|_{p,\Omega} \leq C|\Delta|^{k+1-\alpha-\beta}|f|_{k+1,p,\Omega}, \qquad 0 \leq \alpha + \beta \leq k+1.$$

Here $|\Delta|$ is the diameter of the largest triangle in the triangulation Δ of the domain Ω. In a hierarchical context $|\Delta|$ will become smaller and smaller with each resolution level. We will exploit this fact to prove that a lot of coefficients in a hierarchical surface representation can be neglected which yields the surface compression.

The outline of the paper is as follows. Section 2 is devoted to the idea of hierarchical bases and we discuss their usefulness for compression purposes. In Section 3 we recall some general concepts of polynomials on triangles and we review the relevant aspects and properties of a normalized B-spline basis for Powell–Sabin splines. In Section 4 we show how to construct a stable quasi-interpolation scheme for our normalized B-spline basis which achieves optimal approximation order. Sections 5 and 6 are devoted to the construction of a hierarchical basis, while Section 7 goes into the details of the compression algorithm. Section 8 demonstrates the compression algorithm with some numerical examples, and we conclude the paper with an application to image compression.

2 Hierarchical Bases

The starting point for the idea of hierarchical bases is a nested sequence of finite dimensional spaces of real–valued functions

$$V^0 \subset V^1 \subset V^2 \subset \ldots \subset V^l.$$

As j increases, the resolution of functions in V^j increases. Each space V^j has a finite basis and a set of functions

$$\boldsymbol{\mathcal{B}} := \bigcup_{j=0}^{l} \left\{ \mathcal{B}_i^j \right\}_{i=1}^{n_j} \tag{2.1}$$

is a *hierarchical basis* for V^l given that

$$\boldsymbol{\mathcal{B}}^m := \bigcup_{j=0}^{m} \left\{ \mathcal{B}_i^j \right\}_{i=1}^{n_j} \tag{2.2}$$

is a basis for V^m for each $m = 0, 1, \ldots, l$. Then every $s \in V^l$ can be written in the form

$$s = \sum_{j=0}^{l} \sum_{i=1}^{n_j} c_i^j \mathcal{B}_i^j, \tag{2.3}$$

and the partial sums

$$s_m = \sum_{j=0}^{m} \sum_{i=1}^{n_j} c_i^j \mathcal{B}_i^j, \tag{2.4}$$

are functions in the spaces V^m for each $m = 0, 1, \ldots, l$. The hierarchical expansion (2.3) is especially useful when the partial sums $s_0, s_1, \ldots, s_{l-1}$ can be regarded as better and better approximations of s, i.e.

$$\|s - s_0\| > \|s - s_1\| > \ldots > \|s - s_{l-1}\|.$$

Now we can approximate s at different levels of detail by eliminating the "finer" coefficients. For example, the coarsest approximation s_0 only uses the coefficients $\left\{c_i^0\right\}_{i=1}^{n_0}$.

Suppose that for all m the basis functions $\boldsymbol{\mathcal{B}}^m$ form a stable basis for V^m, i.e. that there exist constants k_1 and k_2 such that for all choices of the coefficient vector $\mathbf{c}^m$

$$k_1 \|\mathbf{c}^m\| \leq \|\boldsymbol{\mathcal{B}}^m \mathbf{c}^m\| \leq k_2 \|\mathbf{c}^m\|, \tag{2.5}$$

then (2.5) expresses that small changes in the size of the coefficients in (2.3) lead to small changes in the size of $\|s\|$. Hence the expansion (2.3) can be used for *compression*.

3 Powell–Sabin splines

We are interested in the spline space $S_2^1(\Delta_{PS})$, that is the space of piecewise quadratic C^1 continuous functions on a Powell–Sabin refinement Δ_{PS}. In this section we briefly review the B-spline representation, the geometric interpretation with control triangles and the stability of the basis.

Consider a triangle $\mathcal{T}(V_1, V_2, V_3)$ in a plane with vertices V_i, $i = 1, 2, 3$. Define $\mathcal{P}_2$ as the space of bivariate polynomials of total degree ≤ 2, then each polynomial $P_2(x, y) \in \mathcal{P}_2$ on $\mathcal{T}$ has a unique representation

$$P_2(x, y) = \sum_{|\lambda|=2} b_\lambda B_\lambda^2(\tau), \tag{3.1}$$

with $\lambda = (\lambda_1, \lambda_2, \lambda_3)$, $\lambda_i \geq 0$ a multi–index of length $|\lambda| = \lambda_1 + \lambda_2 + \lambda_3 = 2$, $\tau = (\tau_1, \tau_2, \tau_3)$ the barycentric coordinates of (x, y) with respect to $\mathcal{T}$, and

$$B_\lambda^2(\tau) = \frac{2!}{\lambda_1! \lambda_2! \lambda_3!} \tau_1^{\lambda_1} \tau_2^{\lambda_2} \tau_3^{\lambda_3} \tag{3.2}$$

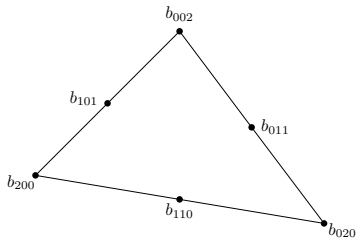

Figure 1: Positions of the Bézier ordinates.

the Bernstein–Bézier polynomials of degree 2 on the triangle [4]. The coefficients b_λ are called the Bézier ordinates. The points $(\frac{\lambda}{2}, b_\lambda)$ are the control points for the surface $z = P_2(x, y)$ and the piecewise linear interpolant to these points is the Bézier net or control net. We can display this Bernstein–Bézier representation schematically, as in Figure 1. The points $\frac{\lambda}{2}$, marked with dots on the figure, are called the Bézier domain points.

Consider a simply connected subset $\Omega \subset \mathbb{R}^2$ with polygonal boundary $\delta\Omega$. Suppose we have a conforming triangulation Δ of Ω, consisting of triangles $\mathcal{T}_j$, $j = 1, \ldots, t$, and having vertices V_i with Cartesian coordinates (x_i, y_i), $i = 1, \ldots, n$. The Powell–Sabin refinement Δ_{PS} of Δ divides each triangle $\mathcal{T}_j$ into six subtriangles with a common vertex. It can be constructed as follows (see Figure 2a):

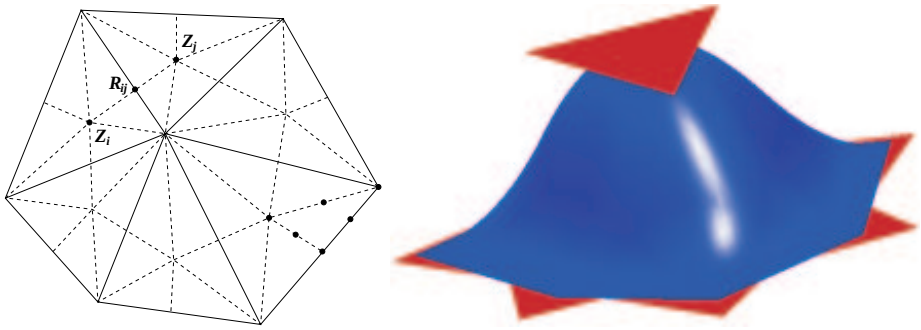

(a) a PS-refinement Δ_{PS} (b) a PS B-spline surface with control triangles

Figure 2: B-spline representation for $S_2^1(\Delta_{PS})$.

1. Choose an interior point Z_j for each triangle $\mathcal{T}_j$, so that if two triangles $\mathcal{T}_i$ and $\mathcal{T}_j$ have a common edge, the line joining Z_i and Z_j intersects this common edge at a point R_{ij} between its vertices. We will choose Z_j as the incenter of triangle $\mathcal{T}_j$.
2. Join the points Z_j to the vertices of $\mathcal{T}_j$.
3. For each edge of $\mathcal{T}_j$
   - which belongs to the boundary $\delta\Omega$, join Z_j to the middle point of the edge.
   - which is common to a triangle $\mathcal{T}_i$, join Z_j to R_{ij}.

Now we consider the space of piecewise quadratic C^1 continuous polynomials on Ω, the Powell–Sabin splines. Each of the $6t$ triangles resulting from the PS-refinement becomes the domain triangle of a quadratic Bernstein–Bézier polynomial (3.1) as indicated for one subtriangle in Figure 2a. Powell and Sabin [10] showed that the following interpolation problem:

$$s(V_k) = f_k, \quad D_x s(V_k) = D_x f_k, \quad D_y s(V_k) = D_y f_k, \quad k = 1, \ldots, n \tag{3.3}$$

has a unique solution $s(x,y)$ in $S_2^1(\Delta_{PS})$. Hence, the dimension of the space $S_2^1(\Delta_{PS})$ equals $3n$.

Dierckx [3] presented a normalized B-spline representation for Powell–Sabin splines

$$s(x,y) = \sum_{i=1}^{n} \sum_{j=1}^{3} c_{ij} B_{ij}(x,y) \quad , \quad (x,y) \in \Omega \tag{3.4}$$

where the B-splines form a convex partition of unity on Ω, i.e.

$$B_{ij}(x,y) \geq 0 \text{ for all } x,y \in \Omega, \tag{3.5}$$

$$\sum_{i=1}^{n} \sum_{j=1}^{3} B_{ij}(x,y) = 1 \text{ for all } x,y \in \Omega. \tag{3.6}$$

Furthermore these basis functions have local support: $B_{ij}(x,y)$ vanishes outside the so-called molecule M_i of vertex V_i, which is the union of all triangles $\mathcal{T}_k$ containing V_i.

The basis functions $B_{ij}(x,y)$ can be obtained as follows: find three linearly independent triplets $(\alpha_{ij}, \beta_{ij}, \gamma_{ij})$, $j = 1,2,3$ for each vertex V_i. $B_{ij}(x,y)$ is the unique solution of the interpolation problem (3.3) with $(f_k, f_{xk}, f_{yk}) = (\delta_{ki}\alpha_{ij}, \delta_{ki}\beta_{ij}, \delta_{ki}\gamma_{ij})$, where δ_{ki} is the Kronecker delta.

The triplets $(\alpha_{ij}, \beta_{ij}, \gamma_{ij})$, $j = 1,2,3$, must be determined in such a way that equations (3.5) and (3.6) are satisfied. To find appropriate triplets $(\alpha_{ij}, \beta_{ij}, \gamma_{ij})$, $j = 1,2,3$, we use the algorithm from [3].

1. For each vertex V_i, find its PS-triangle points. These are the immediately surrounding Bézier domain points of the vertex V_i and vertex V_i itself. Figure 3 shows the PS-triangle points $L, \tilde{L}, L'$ and V_1 for the vertex V_1 in the triangle $\mathcal{T}(V_1, V_2, V_3)$.

2. For each vertex V_i, find a triangle $t_i(Q_{i1}, Q_{i2}, Q_{i3})$ which contains all the PS-triangle points of V_i from all the triangles $\mathcal{T}_k$ in the molecule M_i. These triangles t_i, $i = 1, \ldots, n$ are called PS-triangles and we denote their vertices with $Q_{ij}(X_{ij}, Y_{ij})$. Figure 3 also shows such a PS-triangle t_1.

3. Three linearly independent triplets of real numbers $(\alpha_{ij}, \beta_{ij}, \gamma_{ij})$, $j = 1,2,3$ can be derived from the PS-triangle t_i of a vertex V_i as follows:

$$(\alpha_{i1}, \alpha_{i2}, \alpha_{i3}) \text{ are the barycentric coordinates of } V_i \text{ with respect to } t_i, \tag{3.7}$$

$$(\beta_{i1}, \beta_{i2}, \beta_{i3}) = \left(\frac{Y_{i2} - Y_{i3}}{h}, \frac{Y_{i3} - Y_{i1}}{h}, \frac{Y_{i1} - Y_{i2}}{h} \right), \tag{3.8}$$

$$(\gamma_{i1}, \gamma_{i2}, \gamma_{i3}) = \left(\frac{X_{i3} - X_{i2}}{h}, \frac{X_{i1} - X_{i3}}{h}, \frac{X_{i2} - X_{i1}}{h} \right), \tag{3.9}$$

where

$$h = \begin{vmatrix} X_{i1} & Y_{i1} & 1 \\ X_{i2} & Y_{i2} & 1 \\ X_{i3} & Y_{i3} & 1 \end{vmatrix}.$$

This allows to define the useful notion of control triangles. First, we define with the notation introduced above the PS-control points as

$$C_{ij}(X_{ij}, Y_{ij}, c_{ij}). \tag{3.10}$$

For fixed i, they constitute a triangle $T_i(C_{i1}, C_{i2}, C_{i3})$ that is tangent to the surface at $(V_i, s(V_i))$, see Figure 2b. The projection of the control triangles T_i in the (x,y) plane are the PS-triangles t_i. It is easily verified that

$$A_{t_i} := \text{Area}(t_i(Q_{i1}, Q_{i2}, Q_{i3})) = \frac{1}{2|\beta_{i1}\gamma_{i2} - \gamma_{i1}\beta_{i2}|} = \frac{|f|}{2}. \tag{3.11}$$

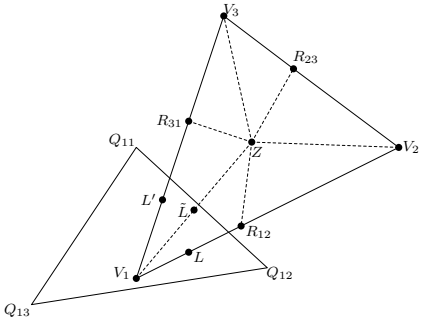

Figure 3: PS-triangle points and PS-triangle.

Obviously there are infinitely many possibilities for a PS-triangle because the only condition is that it contains the appropriate PS-triangle points. It is important to choose small PS-triangles in the construction of the basis functions. The control points will be closer to the surface, which gives the user more local control, and the stability of the basis will be better. Therefore Definition 3.1 introduces a constant K that reflects the influence of the size of the PS-triangles. One can always find PS-triangles that satisfy $K = 1$, and in practice K will be typically smaller than 1. If PS-triangles with minimal area are used, then K can be bounded in function of the smallest angle in the triangulation. For more information we refer to [9].

Definition 3.1. Let D_i be the smallest disk with vertex V_i as center that contains all the PS-triangle points of V_i as in Figure 4 and denote its radius as r_i. An equilateral triangle t_{D_i} with barycenter V_i and inradius $K_i r_i$ with $K_i \geq 1$ obviously is a valid PS-triangle for V_i. We choose the value K_i such that this equilateral triangle contains the actual PS-triangle t_i. Define $K = \max_i K_i$ as the maximum of all constants K_i in the vertices V_i of Δ.

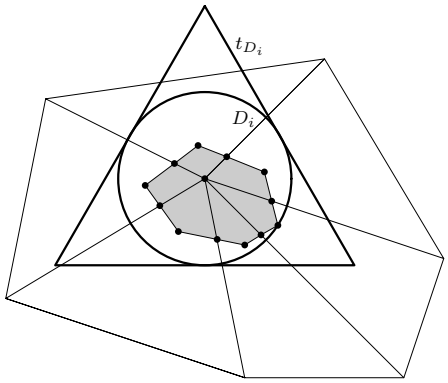

Figure 4: The disk D_i and an equilateral triangle t_{D_i} for $K = 1$.

We recall that the normalized B-spline basis is a stable basis. The set $\{B_{ij}(x, y)\}$ is a stable basis if it satisfies (2.5). The following theorem gives explicit expressions for the constants k_1 and k_2 in (2.5).

Theorem 3.2. *Consider a triangulation Δ of a subset $\Omega \in \mathbb{R}^2$ with polygonal boundary $\delta\Omega$. Suppose Δ is constituted of triangles $\mathcal{T}_j$, $j = 1, \ldots, t$, which have vertices V_i, $i = 1, \ldots, n$. Define Δ_{PS} as the PS-refinement of Δ. Then there exists a constant k_1 such that for all Powell–Sabin splines $s(x, y) \in S_2^1(\Delta_{PS})$ in their normalized B-spline representation (3.4),*

$$k_1 \|\mathbf{c}\|_\infty \leq \|s(x, y)\|_\infty \leq \|\mathbf{c}\|_\infty,$$

with $\|\mathbf{c}\|_\infty := \max_{ij} |c_{ij}|$, $\|f\|_\infty := \max_\Omega |f(x,y)|$ *and*

$$k_1 = \left[1 + \frac{384\sqrt{3}K}{\sin(\theta_\Delta \sin(\theta_\Delta)/4)^4 \tan(\theta_\Delta \sin(\theta_\Delta)/8)}\right]^{-1}.$$

Here θ_Δ *is the smallest angle in the triangulation* Δ *and* K *is the constant defined in Definition 3.1.*

Proof. For the proof we refer to the work of Maes *et al.* [9]. □

4 Approximation power of Powell–Sabin B-splines

The main result of this section is Theorem 4.6 which states the existence of a linear quasi-interpolation operator Q which maps $C(\Omega)$ onto the spline space $S_2^1(\Delta_{PS})$ in such a way that if f lies in a Sobolev space $W_p^{k+1}(\Omega)$ with $1 \le k \le 2$ and $2 \le p \le \infty$, then Qf approximates f and its derivatives to optimal order.

First we introduce some notations that will be used in this section, and we collect some properties of triangulations and Powell–Sabin refinements. Suppose Δ is a triangulation of a subset $\Omega \in \mathbb{R}^2$ with a PS-refinement Δ_{PS}, and $\mathcal{T}$ is a triangle. With $|\mathcal{T}|$ we mean the diameter of the smallest disk containing $\mathcal{T}$, and $\rho_\mathcal{T}$ will denote the radius of the largest disk contained in $\mathcal{T}$. Denote the longest edge of $\mathcal{T}$ with $e_{\max}(\mathcal{T})$. The notations $\theta_\mathcal{T}$, θ_Δ and $\theta_{\Delta_{PS}}$ will be used for the smallest angles in resp. $\mathcal{T}$, Δ, and Δ_{PS}. We give some estimates for the introduced quantities.

Property 4.1.

$$\frac{|\mathcal{T}|}{\rho_\mathcal{T}} \le \frac{4}{\tan(\theta_\mathcal{T}/2)}.$$

Proof. It is well–known that

$$\rho_\mathcal{T} = \tan(\theta_\mathcal{T}/2) \cdot \frac{a+b-c}{2},$$

with a, b and c the side lengths of the triangle. Side length c corresponds to the side opposite to the angle $\theta_\mathcal{T}$, and thus has the smallest value. The following inequalities hold:

$$\frac{2}{\tan(\theta_\mathcal{T}/2)} = \frac{a+b-c}{\rho_\mathcal{T}} \ge \frac{|e_{\max}(\mathcal{T})|}{\rho_\mathcal{T}} \ge \frac{|\mathcal{T}|/2}{\rho_\mathcal{T}}.$$

□

Property 4.2.

$$\theta_{\Delta_{PS}} \ge \theta_\Delta \sin(\theta_\Delta)/4$$

Proof. We refer to the work of Lai and Schumaker [7]. □

We will consider complex valued functions on a bounded domain R in the 2 dimensional Euclidean space $\mathbb{R}^2$. Let α and β denote positive integers. We define $L_p(R)$ as the set of functions f such that $\int_R |f(x)|^p dx$ exists and is finite. For the case $p = \infty$ we define $L_\infty(R)$ as the set of functions f such that $\max_{(x,y)\in R} |f(x,y)| < \infty$. The norm on $L_p(R)$ is given by $\|f\|_{p,R} = \left(\int_R |f(x)|^p\right)^{1/p}$ and the norm on $L_\infty(R)$ by $\|f\|_{\infty,R} = \max_{(x,y)\in R} |f(x,y)|$. By $W_p^k(R)$ we mean the usual Sobolev space, i.e. the set of all functions in $L_p(R)$ whose distributional derivatives of order less than or equal to k are in $L_p(R)$. The norm on $W_p^k(R)$ is $\|f\|_{k,p,R} = \sum_{\alpha+\beta\le k} \|D_x^\alpha D_y^\beta f\|_{p,R}$. We will also use the semi–norm $|f|_{k,p,R} = \sum_{\alpha+\beta=k} \|D_x^\alpha D_y^\beta f\|_{p,R}$. For an excellent survey concerning Sobolev spaces the reader is referred to [1].

Before we prove the main theorem, we introduce three helpful lemmas. The first lemma bounds the size of the PS-triangles in function of the constant K defined before. The second lemma is a form of Markov inequality for polynomials in $\mathcal{P}_2$ (3.1). The third lemma is the well-known Bramble–Hilbert lemma [2] which we state without proof for the specific case of functions in $\mathbb{R}^2$.

Lemma 4.3. *Denote the PS-triangle point with the longest distance to vertex V_i as S and define $\mathcal{T}_S \in \Delta_{PS}$ as either one of the two triangles that contains the PS-triangle point S. Then*

$$\frac{|e_{\max}(t_i)|}{|e_{\max}(\mathcal{T}_S)|} \leq \sqrt{3}K,$$

with K the constant introduced in Definition 3.1 and t_i the PS-triangle in vertex V_i.

Proof. By the definition of K there exists an equilateral triangle t_{D_i} that contains the PS-triangle t_i. Hence it is sufficient to prove that

$$\frac{|e_{\max}(t_{D_i})|}{|e_{\max}(\mathcal{T}_S)|} \leq \sqrt{3}K.$$

Denote r_i as the radius of the disk D_i, defined in Definition 3.1. Then

$$|e_{\max}(t_{D_i})| = 2\sqrt{3}K_i r_i \leq 2\sqrt{3}Kr_i.$$

If we combine this inequality with the fact that

$$|e_{\max}(\mathcal{T}_S)| \geq 2|SV_i| = 2r_i,$$

then we have proven the lemma. □

Lemma 4.4. *Suppose $s(x,y) \in S_2^1(\Delta_{PS})$ and let $1 \leq p \leq \infty$. Consider a triangle $\mathcal{T}_{PS}$ in the PS-refinement Δ_{PS} of Δ. Then there exists a constant C_1 such that*

$$\|D_x^\alpha D_y^\beta s(x,y)\|_{p,\mathcal{T}_{PS}} \leq \frac{C_1}{\rho_{\mathcal{T}_{PS}}^{\alpha+\beta}} \|s(x,y)\|_{p,\mathcal{T}_{PS}}, \qquad 0 \leq \alpha+\beta \leq 2,$$

with $\rho_{\mathcal{T}_{PS}}$ the radius of the largest disk contained in $\mathcal{T}_{PS}$.

Proof. This follows immediately from Lemma 4.2 in [6]. □

Lemma 4.5 (Bramble–Hilbert [2]). *Let R be a bounded domain in $\mathbb{R}^2$ with diameter $|R|$, let f be a function in $W_p^k(R)$, and let F be a linear functional on $C^j(R)$ such that $0 \leq j < k$ satisfying*

1. *$|F(f)| \leq G \sum_{l=0}^{j} |R|^l |f|_{l,R}$ where G is independent of $|R|$ and f and*

$$|f|_{l,R} = \sup_{(x,y)\in R} \sum_{\alpha+\beta=l} |D_x^\alpha D_y^\beta f(x,y)|,$$

2. *$F(q) = 0$ for all $q \in \{p(x,y) \mid D_x^\alpha D_y^\beta p(x,y) = 0,\ \alpha+\beta = k\}$.*

Then for $p > 2/(k-j)$ there is a constant G_1 independent of $|R|$ and f such that

$$|F(f)| \leq G_1 |R|^{k-2/p} |f|_{k,p,R}.$$

We will now prove that the best order of approximation by normalized Powell–Sabin B-splines is even achieved by a linear quasi-interpolation operator.

Theorem 4.6. *Consider a triangulation Δ of a subset $\Omega \in \mathbb{R}^2$ with polygonal boundary $\delta\Omega$. Suppose Δ is constituted of triangles $\mathcal{T}_j$, $j = 1,\ldots,t$, which have vertices V_i, $i = 1,\ldots,n$. Define Δ_{PS} as the PS-refinement of Δ. Fix $1 \leq k \leq 2$ and $2 \leq p \leq \infty$. Then there exists a linear quasi-interpolation operator Q mapping $C(\Omega)$ onto $S_2^1(\Delta_{PS})$ such that Qf is in normalized B-spline representation (3.4) and for every $f \in W_p^{k+1}(\Omega)$,*

$$\|D_x^\alpha D_y^\beta (f - Qf)\|_{p,\Omega} \leq C|\Delta|^{k+1-\alpha-\beta} |f|_{k+1,p,\Omega},$$

for all $0 \leq \alpha+\beta \leq k+1$. Here $|\Delta|$ is the maximum of the diameters of the triangles in Δ and C is a constant. If $\alpha > 0$ or $\beta > 0$ then C depends upon the smallest angle θ_Δ in the triangulation Δ.

Proof. From (3.4) and the construction of the B-spline basis we have

$$\begin{bmatrix} s(V_i) \\ s_x(V_i) \\ s_y(V_i) \end{bmatrix} = A \begin{bmatrix} c_{i1} \\ c_{i2} \\ c_{i3} \end{bmatrix} \qquad \text{with} \qquad A = \begin{bmatrix} \alpha_{i1} & \alpha_{i2} & \alpha_{i3} \\ \beta_{i1} & \beta_{i2} & \beta_{i3} \\ \gamma_{i1} & \gamma_{i2} & \gamma_{i3} \end{bmatrix}.$$

This allows to define a quasi-interpolant Q of the form

$$Qf = \sum_{i=1}^{n} \sum_{j=1}^{3} \mu_{ij}(f) B_{ij},$$

with

$$\begin{bmatrix} \mu_{i1}(f) \\ \mu_{i2}(f) \\ \mu_{i3}(f) \end{bmatrix} := A^{-1} \begin{bmatrix} f(V_i) \\ f_x(V_i) \\ f_y(V_i) \end{bmatrix}.$$

Clearly the operator Q satisfies

$$\begin{aligned} Qs = s, \qquad & \forall s \in S_2^1(\Delta_{PS}), \\ Qf(V_i) = f(V_i), \qquad & i = 1, \ldots, n, \\ \nabla Qf(V_i) = \nabla f(V_i), \qquad & i = 1, \ldots, n. \end{aligned}$$

If we take into account that $\alpha_{i3} = 1 - \alpha_{i1} - \alpha_{i2}$, $\beta_{i3} = -\beta_{i1} - \beta_{i2}$ and $\gamma_{i3} = -\gamma_{i1} - \gamma_{i2}$, then we find that the inverse of A is equal to

$$A^{-1} = \begin{bmatrix} 1 & \eta_{i1} & \tilde{\eta}_{i1} \\ 1 & \eta_{i2} & \tilde{\eta}_{i2} \\ 1 & \eta_{i3} & \tilde{\eta}_{i3} \end{bmatrix},$$

with

$$\begin{aligned} \eta_{ij} &:= \frac{\alpha_{i2}\gamma_{i1} - \alpha_{i1}\gamma_{i2} + \delta_{j1}\gamma_{i2} - \delta_{j2}\gamma_{i1}}{\beta_{i1}\gamma_{i2} - \beta_{i2}\gamma_{i1}}, \\ \tilde{\eta}_{ij} &:= \frac{\alpha_{i1}\beta_{i2} - \alpha_{i2}\beta_{i1} - \delta_{j1}\beta_{i2} + \delta_{j2}\beta_{i1}}{\beta_{i1}\gamma_{i2} - \beta_{i2}\gamma_{i1}}. \end{aligned}$$

Fix (x, y) in a triangle $\mathcal{T}_{PS} \in \Delta_{PS}$ with $\mathcal{T}_{PS}$ a subtriangle of triangle $\mathcal{T} \in \Delta$. By the stability of the normalized B-spline basis for $S_2^1(\Delta_{PS})$,

$$|Qf(x,y)| \leq \sum_{i|V_i \in \mathcal{T}} \sum_{j=1}^{3} |\mu_{ij}(f)| B_{ij}(x,y) \leq \max_{i|V_i \in \mathcal{T}, j} |f(V_i) + \eta_{ij} f_x(V_i) + \tilde{\eta}_{ij} f_y(V_i)|. \tag{4.1}$$

We can find upper bounds for η_{ij} and $\tilde{\eta}_{ij}$ by using the fact that $|\alpha_{ij}| \leq 1$ (3.7) and $|\delta_{ij}| \leq 1$, and by using the explicit formulas for β_{ij} and γ_{ij} given in (3.8) and (3.9)

$$|\eta_{ij}| \leq |\alpha_{i2}\gamma_{i1} - \alpha_{i1}\gamma_{i2} + \delta_{j1}\gamma_{i2} - \delta_{j2}\gamma_{i1}| 2A_{t_i} \leq 2(|X_{i3} - X_{i2}| + |X_{i1} - X_{i3}|) \leq 4|e_{\max}(t_i)|.$$

Similarly we find that $\tilde{\eta}_{ij} \leq 4|e_{\max}(t_i)|$, and in combination with Lemma 4.3 we find

$$\begin{array}{rcccl} |\eta_{ij}| & \leq & 4\sqrt{3}K|e_{\max}(\mathcal{T}_S)| & \leq & 4\sqrt{3}K|\mathcal{T}| \\ |\tilde{\eta}_{ij}| & \leq & 4\sqrt{3}K|e_{\max}(\mathcal{T}_S)| & \leq & 4\sqrt{3}K|\mathcal{T}|, \end{array} \tag{4.2}$$

with $|\mathcal{T}|$ the diameter of triangle $\mathcal{T}$ and $\mathcal{T}_S$ the subtriangle of $\mathcal{T}$ as defined in Lemma 4.3. By substituting the upper bounds for η_{ij} and $\tilde{\eta}_{ij}$ in equation (4.1) we find that

$$|Qf(x,y)| \leq \|f\|_{\infty,\mathcal{T}} + 4\sqrt{3}K|\mathcal{T}| \sup_{(x,y)\in\mathcal{T}} (|f_x(x,y)| + |f_y(x,y)|).$$

This immediately implies the existence of a constant C_2 such that

$$|Qf(x,y) - f(x,y)| \leq C_2 \sum_{l=0}^{1} |\mathcal{T}|^l |f|_{l,\mathcal{T}},$$

with $|f|_{l,\mathcal{T}}$ defined as in Lemma 4.5. The Bramble–Hilbert lemma implies

$$|Qf(x,y) - f(x,y)| \leq C_3 |\mathcal{T}|^{k+1-2/p} |f|_{k+1,p,\mathcal{T}}.$$

We find that

$$\begin{aligned}
\|Qf(x,y) - f(x,y)\|_{p,\mathcal{T}} &= \left(\int_{\mathcal{T}} |Qf(x,y) - f(x,y)|^p dxdy \right)^{1/p} \\
&\leq C_3 |\mathcal{T}|^{k+1-2/p} |f|_{k+1,p,\mathcal{T}} \cdot (\text{Area}(\mathcal{T}))^{1/p} \\
&\leq C_3 |\mathcal{T}|^{k+1-2/p} |f|_{k+1,p,\mathcal{T}} \cdot \left(\pi |\mathcal{T}|^2\right)^{1/p} \\
&= C_4 |\mathcal{T}|^{k+1} |f|_{k+1,p,\mathcal{T}}.
\end{aligned}$$

This establishes the theorem for $\alpha = \beta = 0$ and $p = \infty$. For $2 \leq p < \infty$ we have that

$$\begin{aligned}
\|Qf(x,y) - f(x,y)\|_{p,\Omega} &= \left(\sum_{\mathcal{T} \in \Omega} \|Qf(x,y) - f(x,y)\|_{p,\mathcal{T}}^p \right)^{1/p} \\
&\leq C_4 |\Delta|^{k+1} \left(\sum_{\mathcal{T} \in \Omega} |f|_{k+1,p,\mathcal{T}}^p \right)^{1/p} \\
&= C_4 |\Delta|^{k+1} \left(\sum_{\mathcal{T} \in \Omega} \left(\sum_{\alpha+\beta=k+1} \|D_x^\alpha D_y^\beta f\|_{p,\mathcal{T}} \right)^p \right)^{1/p} \\
&\leq C_4 |\Delta|^{k+1} (k+2) \left(\sum_{\mathcal{T} \in \Omega} \max_{\alpha,\beta | \alpha+\beta=k+1} \|D_x^\alpha D_y^\beta f\|_{p,\mathcal{T}}^p \right)^{1/p} \\
&\leq C_4 |\Delta|^{k+1} 4 \left(\sum_{\mathcal{T} \in \Omega} \sum_{\alpha+\beta=k+1} \|D_x^\alpha D_y^\beta f\|_{p,\mathcal{T}}^p \right)^{1/p} \\
&= C_5 |\Delta|^{k+1} |f|_{k+1,p,\Omega}.
\end{aligned}$$

These equations establish the theorem for $\alpha = \beta = 0$ and for arbitrary $p \geq 2$.

Fix $0 \leq \alpha + \beta \leq k+1$. Applying Lemma 4.4 to the polynomial $(Qf)|_{\mathcal{T}_{PS}}$ gives

$$\|D_x^\alpha D_y^\beta Qf\|_{p,\mathcal{T}_{PS}} \leq \frac{C_1}{\rho_{\mathcal{T}_{PS}}^{\alpha+\beta}} \|Qf\|_{p,\mathcal{T}_{PS}}. \tag{4.3}$$

Let e and $\tilde{e}$ be two edges of an arbitrary subtriangle of $\mathcal{T}$. Then

$$\sin(\theta_{\Delta_{PS}}) |e| \leq |\tilde{e}|.$$

If we want to compare two arbitrary edges e_1 and e_2 of two arbitrary subtriangles of triangle $\mathcal{T} \in \Delta$, then there always exists a series of maximum five edges from e_1 to e_2 such that each pair of successive edges in the series has a common subtriangle in $\mathcal{T}$, hence

$$|e_1| \leq \left(\frac{1}{\sin(\theta_{\Delta_{PS}})} \right)^4 |e_2|.$$

If we apply this to (4.2), we find that

$$\begin{aligned} |\eta_{ij}| &\leq \frac{4\sqrt{3}K}{\sin(\theta_{\Delta_{PS}})^4}|\mathcal{T}_{PS}| \\ |\tilde{\eta}_{ij}| &\leq \frac{4\sqrt{3}K}{\sin(\theta_{\Delta_{PS}})^4}|\mathcal{T}_{PS}|, \end{aligned}$$

with $|\mathcal{T}_{PS}|$ the diameter of triangle $\mathcal{T}_{PS}$. Combining (4.1) and (4.3) with these upper bounds yields

$$|D_x^\alpha D_y^\beta Qf(x,y)| \leq \frac{C_1}{\rho_{\mathcal{T}_{PS}}^{\alpha+\beta}} \left[\|f\|_{\infty,\mathcal{T}} + \frac{4\sqrt{3}K}{\sin(\theta_{\Delta_{PS}})^4}|\mathcal{T}_{PS}| \sup_{(x,y)\in\mathcal{T}} (|f_x(x,y)| + |f_y(x,y)|) \right],$$

and we find that

$$|D_x^\alpha D_y^\beta (Qf - f)(x,y)| \leq \frac{C_6}{\rho_{\mathcal{T}_{PS}}^{\alpha+\beta}} \sum_{l=0}^{1} |\mathcal{T}_{PS}|^l |f|_{l,\mathcal{T}} \leq \frac{C_6}{\rho_{\mathcal{T}_{PS}}^{\alpha+\beta}} \sum_{l=0}^{1} |\mathcal{T}|^l |f|_{l,\mathcal{T}},$$

where C_6 depends on the smallest angle $\theta_{\Delta_{PS}}$ in Δ_{PS}. The Bramble–Hilbert theorem implies that

$$|D_x^\alpha D_y^\beta (Qf - f)(x,y)| \leq \frac{C_7}{\rho_{\mathcal{T}_{PS}}^{\alpha+\beta}} |\mathcal{T}|^{k+1-2/p} |f|_{k+1,p,\mathcal{T}}. \tag{4.4}$$

From Property 4.1 we get that

$$\frac{1}{\rho_{\mathcal{T}_{PS}}} \leq \frac{4}{\tan(\theta_{\Delta_{PS}}/2)|\mathcal{T}_{PS}|} \tag{4.5}$$

and it is an easy exercise to prove that there exists a constant C_8 which depends only on the smallest angle $\theta_{\Delta_{PS}}$ in Δ_{PS} such that

$$|\mathcal{T}_{PS}| \geq C_8 |\mathcal{T}|. \tag{4.6}$$

Equations (4.4), (4.5) and (4.6) and Property 4.2 together yield

$$|D_x^\alpha D_y^\beta (Qf - f)(x,y)| \leq C_9 |\mathcal{T}|^{k+1-\alpha-\beta-2/p} |f|_{k+1,p,\mathcal{T}},$$

with C_9 a constant dependent only on θ_Δ. An analogous derivation as above proves the theorem for $0 \leq \alpha + \beta \leq k+1$ and $2 \leq p \leq \infty$. □

5 Triadic refinement

We discuss a triadic scheme for refining a given triangulation Δ and its associated PS-refinement Δ_{PS} to produce nested sequences

$$\Delta^0 \subset \Delta^1 \subset \Delta^2 \subset \ldots \subset \Delta^l \tag{5.1}$$

and

$$\Delta_{PS}^0 \subset \Delta_{PS}^1 \subset \Delta_{PS}^2 \subset \ldots \subset \Delta_{PS}^l. \tag{5.2}$$

In the next section we review a subdivision scheme to compute a representation (3.4) of a Powell–Sabin spline on a triadic refinement Δ^{j+1} of a triangulation Δ^j [12].

Algorithm 5.1. *Let Δ_{PS}^0 be the PS-refinement associated with a triangulation Δ^0. For each triangle $\mathcal{T}$ in Δ^0,*

1. *add a new vertex V_{ijk} such that this new vertex coincides with the interior vertex Z_{ijk} of the PS-refinement Δ_{PS},*

2. *insert two new vertices on the edges each at one side of the R_{ij} and connect these vertices such that they form a hexagon. These new vertices have to be chosen in such a way that the resulting hexagon contains the interior vertex V_{ijk},*

3. *connect the six new vertices on the edges with the interior vertex V_{ijk},*

4. *for each of the nine new triangles, a new interior point is determined on the line of the old PS-refinement Δ^0_{PS} that crosses the new triangle.*

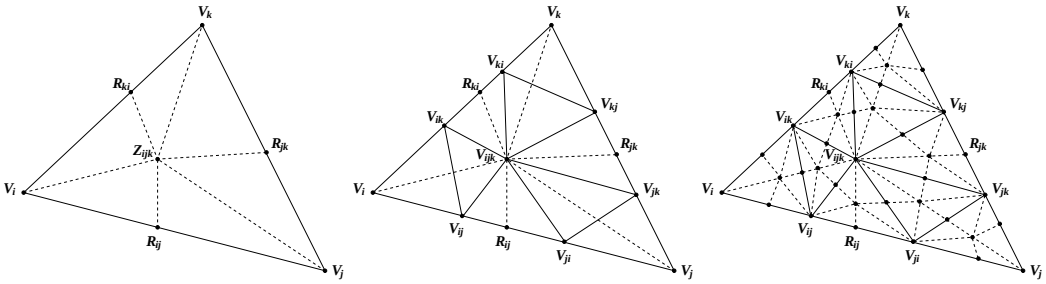

(a) (b) (c)

Figure 5: Principle of triadic subdivision. We place a new vertex at the position of the interior point Z_{ijk} and two new vertices on the edges each at one side of the R_{ij}.

The steps of the algorithm are illustrated in Figure 5. It is clear that Algorithm 5.1 splits each triangle in Δ^0 into nine subtriangles. This process can be repeated as often as desired to produce the nested sequences in (5.1) and (5.2).

Let $\mathcal{V}^j$, $\mathcal{E}^j$ and $\mathcal{T}^j$ denote the number of vertices, edges and triangles in the triangulation Δ^j obtained after j steps of Algorithm 5.1 on an initial triangulation Δ^0. Then the following equations can be deduced from Algorithm 5.1:

$$\begin{aligned} \mathcal{T}^j &= 9\mathcal{T}^{j-1}, \\ \mathcal{V}^j &= \mathcal{V}^{j-1} + 2\mathcal{E}^{j-1} + \mathcal{T}^{j-1}, \end{aligned}$$

and from Euler's formula we get that

$$\mathcal{E}^j = \mathcal{V}^{j-1} + 2\mathcal{E}^{j-1} + 10\mathcal{T}^{j-1} - 1.$$

Property 5.2. *For all $j \geq 0$,*

$$\begin{aligned} \mathcal{T}^j &= 9^j\mathcal{T}^0, \\ \mathcal{E}^j &= 3^{j-1}\mathcal{V}^0 + 2\cdot 3^{j-1}\mathcal{E}^0 - 3^{j-1} + \left(\frac{3}{2}9^j - \frac{7}{6}3^j\right)\mathcal{T}^0, \\ \mathcal{V}^j &= 3^{j-1}\mathcal{V}^0 + 2\cdot 3^{j-1}\mathcal{E}^0 - 3^{j-1} + 1 + \left(\frac{9^j}{2} - \frac{7}{6}3^j\right)\mathcal{T}^0, \end{aligned}$$

Proof. This can easily be proved by induction. □

In Table 1 we give the numbers $\mathcal{T}^j$, $\mathcal{E}^j$, and $\mathcal{V}^j$ for $j = 0, \ldots, 8$, starting from two triangles with one common edge. For completion the table shows also the dimension of $S^1_2(\Delta^j_{PS})$ which is equal to $3 \cdot \mathcal{V}^j$.

j	$\mathcal{T}^j$	$\mathcal{E}^j$	$\mathcal{V}^j$	$\dim S_2^1(\Delta_{PS}^j)$
0	2	5	4	12
1	18	33	16	48
2	162	261	100	300
3	1458	2241	784	2352
4	13122	19845	6724	20172
5	118098	177633	59536	178608
6	1062882	1595781	532900	1598700
7	9565938	14353281	4787344	14362032
8	86093442	129153285	43059844	129179532

Table 1: Number of triangles, edges, vertices and dimension in $S_2^1(\Delta_{PS}^j)$ for $j = 0, \ldots, 8$.

6 A hierarchical basis

It is convenient to write the following in matrix form. Therefore we write a Powell–Sabin spline $s(x, y) \in S_2^1(\Delta_{PS})$ as

$$s(x, y) = \mathbf{\Phi}\mathbf{c},$$

where $\mathbf{\Phi}$ denotes the row vector of basis functions $B_{ij}(x, y)$ and $\mathbf{c}$ the column vector with the coefficients c_{ij}. A superscript j denotes the resolution level as usual.

In [12], Vanraes *et al.* present a subdivision scheme to compute a representation (3.4) of a Powell–Sabin spline on a triadic refinement Δ^{j+1} of a triangulation Δ^j. The result is a denser set of control points $\mathbf{c}^{j+1}$. The corresponding new basis functions $\mathbf{\Phi}^{j+1}$ have smaller support than the basis functions $\mathbf{\Phi}^j$ on the previous level and each of the functions in $\mathbf{\Phi}^j$ can be written as a linear combination of the functions in $\mathbf{\Phi}^{j+1}$, i.e. there exists a matrix $\mathbf{P}^j$ such that

$$\mathbf{\Phi}^j = \mathbf{\Phi}^{j+1}\mathbf{P}^j.$$

We obtain a multiresolution analysis, an increasing sequence of subspaces can be associated with the base triangulation Δ^0. Vanraes *et al.* [12] give formula to compute the refined control points. The result can be written in block matrix form as

$$\mathbf{c}^{j+1} = \begin{bmatrix} \mathbf{O}^j \\ \mathbf{N}^j \end{bmatrix} \mathbf{c}^j.$$

The part $\mathbf{O}^j$ computes new control points for the old vertices that are contained in both Δ^j and Δ^{j+1}, and the part $\mathbf{N}^j$ computes control points for the new vertices that are added when going from Δ^j to Δ^{j+1}. We remark that $\mathbf{O}^j$ is invertible, the new control triangle for an old vertex is in fact only a rescaled version of the old control triangle. Furthermore the subdivsion formula are convex combinations, i.e. the rows of $\mathbf{O}^j$ and $\mathbf{N}^j$ contain a finite number of elements smaller than one and each row sums up to one. This means the subdivision algorithm is stable.

We split $\mathbf{\Phi}^{j+1}$ in functions $\mathcal{O}^{j+1}$ associated with the old vertices in Δ^j and functions $\mathcal{N}^{j+1}$ associated with the new vertices that are added when going from Δ^j to Δ^{j+1}

$$\mathbf{\Phi}^{j+1} = \left[\mathcal{O}^{j+1}\mathcal{N}^{j+1}\right].$$

Define the set of functions $\boldsymbol{\mathcal{B}}^m$ (2.2) as

$$\boldsymbol{\mathcal{B}}^m := \left\{ \mathbf{\Phi}^0 \cup \bigcup_{j=1}^{m} \mathcal{N}^j \right\} \tag{6.1}$$

for each $m = 0, \ldots, l$ and define the set $\boldsymbol{\mathcal{B}}$ as in (2.1).

Theorem 6.1. *For each $0 \leq m \leq l$, the set of splines $\boldsymbol{\mathcal{B}}^m$ (6.1) forms a basis for $S_2^1(\Delta_{PS}^m)$.*

Proof. From the previous we know that

$$\begin{bmatrix} \mathbf{\Phi}^j & \mathcal{N}^{j+1} \end{bmatrix} = \mathbf{\Phi}^{j+1} \begin{bmatrix} \mathbf{O}^j & \mathbf{0} \\ \mathbf{N}^j & \mathbf{1} \end{bmatrix}.$$

Because $\mathbf{O}^j$ is invertible, the matrix $\begin{bmatrix} \mathbf{O}^j & \mathbf{0} \\ \mathbf{N}^j & \mathbf{1} \end{bmatrix}$ is also invertible, and we can write

$$\begin{bmatrix} \left(\mathbf{O}^j\right)^{-1} & \mathbf{0} \\ -\mathbf{N}^j \left(\mathbf{O}^j\right)^{-1} & \mathbf{1} \end{bmatrix} \begin{bmatrix} \mathbf{\Phi}^j & \mathcal{N}^{j+1} \end{bmatrix} = \mathbf{\Phi}^{j+1}.$$

Hence for all j we have proven that the set of functions $\begin{bmatrix} \mathbf{\Phi}^j & \mathcal{N}^{j+1} \end{bmatrix}$ forms a basis for the space V^{j+1}. The theorem follows by induction. □

Theorem 6.1 shows that $\boldsymbol{\mathcal{B}}$ is a hierarchical basis for $S_2^1(\Delta_{PS}^l)$. Every spline $s(x,y) \in S_2^1(\Delta_{PS}^l)$ has a unique hierarchical representation

$$s(x,y) = \sum_{j=0}^{l} \sum_{i=1}^{n_j} c_i^j \mathcal{B}_i^j(x,y), \tag{6.2}$$

with $\mathcal{B}_i^0 := \mathbf{\Phi}_i^0$ and $\mathcal{B}_i^j := \mathcal{N}_i^j, 1 \le j \le l$. The basis functions in Theorem 6.1 are local and stable. Define $M^j(V)$ as the molecule of vertex V in triangulation Δ^j, i.e. the union of all triangles $\mathcal{T}_k \in \Delta^j$ containing vertex V.

Theorem 6.2. *For each $0 \le j \le l$, the supports and sizes of $\mathcal{B}_i^j$ satisfy*

1. $\operatorname{supp} \mathcal{B}_i^j \subseteq M^j(V)$ *if the coefficient c_i^j is associated with vertex $V \in \Delta^j$,*
2. $\mathcal{B}_i^j(x,y) \ge 0$,
3. $\sum_{i=1}^{n_j} \mathcal{B}_i^j(x,y) \le 1$.

Proof. This follows immediately from the construction of the hierarchical basis and from properties (3.5) and (3.6). □

We will now show that the spline $s(x,y)$ in its unique hierarchical representation (6.2) is stable in the sense that if $s(x,y)$ has small coefficients, then $\|s(x,y)\|_\infty$ is also small.

Theorem 6.3. *Suppose $s(x,y) \in S_2^1(\Delta_{PS}^l)$ is a spline in its unique hierarchical representation (6.2) whose coefficients satisfy*

$$|c_i^j| \le \frac{\epsilon}{l+1}.$$

Then $\|s(x,y)\|_\infty \le \epsilon$.

Proof. Fix $(x,y) \in \Omega$, then

$$\begin{aligned} |s(x,y)| &\le \sum_{j=0}^{l} \sum_{i=1}^{n_j} |c_i^j| \mathcal{B}_i^j(x,y) \\ &\le \sum_{j=0}^{l} \frac{\epsilon}{l+1} \sum_{i=1}^{n_j} \mathcal{B}_i^j(x,y) \end{aligned}$$

The claim that $\|s(x,y)\|_\infty \le \epsilon$ follows from property 3 in Theorem 6.2. □

7 Compression

Define $\mathcal{V}_l$ as the set of vertices in Δ^l. Because of (3.3), a spline $s(x,y) \in S_2^1(\Delta_{PS}^l)$ is uniquely determined by the values

$$\bigcup_{V \in \mathcal{V}_l} \{s(V), s_x(V), s_y(V)\}. \tag{7.1}$$

Define Q^m as the linear quasi-interpolation operator mapping $C(\Omega)$ onto $S_2^1(\Delta_{PS}^m)$ as defined in Theorem 4.6, $m = 0, \ldots, l$. Define

$$\hat{s}^0 := Q^0 s(x,y) \tag{7.2}$$

and

$$\hat{s}^m := Q^m \left(s(x,y) - \sum_{j=0}^{m-1} \hat{s}^j \right), \qquad m = 1, \ldots, l. \tag{7.3}$$

We can write $\hat{s}^m$ in matrix form as

$$\mathbf{\Phi}^m \mathbf{c}^m, \qquad m = 0, \ldots, l.$$

As before, let $\mathbf{\Phi}^m = [\mathcal{O}^m \mathcal{N}^m]$ and analogously $\mathbf{c}^m = [\mathbf{c}_o^m \mathbf{c}_n^m]$. It is clear from the construction of $\hat{s}^m$ that the subset of coefficients $\mathbf{c}_o^m$ corresponding to the basisfunctions $\mathcal{O}^m$ are zero for $m = 1, \ldots, l$. This construction can easily be turned into an algorithm for computing the coefficients in (6.2). We refer to this process of computing the coefficients in (6.2) from the values (7.1) as *decomposition*.

Algorithm 7.1 (Decomposition).

1. *Use (7.2) to compute* $\{c_i^0\}_{i=1}^{n_0} \equiv \mathbf{c}^0$ *from (7.1).*
2. *For* $m = 1, \ldots, l$,
   (a) *use (7.3) to form the spline* $\hat{s}^m$ *from (7.1),*
   (b) *compute* $\{c_i^m\}_{i=1}^{n_m} \equiv \mathbf{c}_n^m$.

In view of Theorem 6.3 we can now describe a thresholding strategy.

Algorithm 7.2 (Thresholding).

1. *Choose* ϵ.
2. *For each* $m = 0, \ldots, l$, *drop the coefficients in* $\{c_i^m\}_{i=1}^{n_m}$ *that are smaller than the threshold* ϵ.

Our decomposition algorithm will give good compression rates when the hierarchical expansion (6.2) contains many small coefficients. The following theorem guarantees that the coefficients become smaller with each hierarchic level m.

Theorem 7.3. *Fix* $1 \le k \le 2$ *and* $2 \le p \le \infty$. *Given is a function* $f \in W_p^{k+1}(\Omega)$. *Suppose* $s \in S_2^1(\Delta_{PS}^l)$ *is the unique solution of the interpolation problem (3.3). Then for all* $0 \le m \le l-1$,

$$\|s - s_m\|_{p,\Omega} \le C |\Delta^m|^{k+1} |f|_{k+1,p,\Omega}. \tag{7.4}$$

Here $|\Delta^m|$ *is the maximum of the diameters of the triangles in* Δ^m, *and* C *is a constant.*

Proof. By Theorem 4.6 we have that

$$\|s - f\|_{p,\Omega} \le C_1 |\Delta^l|^{k+1} |f|_{k+1,p,\Omega}$$

and

$$\|f - s_m\|_{p,\Omega} \le C_2 |\Delta^m|^{k+1} |f|_{k+1,p,\Omega}$$

for all m. Then from the triangle inequality we find that

$$\begin{aligned} \|s - s_m\|_{p,\Omega} &\le \|s - f\|_{p,\Omega} + \|f - s_m\|_{p,\Omega} \\ &\le \left(C_1 |\Delta^l|^{k+1} + C_2 |\Delta^m|^{k+1} \right) |f|_{k+1,p,\Omega} \\ &\le (C_1 + C_2) |\Delta^m|^{k+1} |f|_{k+1,p,\Omega}. \end{aligned}$$

Setting $C = C_1 + C_2$ proves the theorem. □

Suppose that $f \in W_p^3(\Omega)$. Then the theorem implies the following: if s is the solution of the interpolation problem (3.3), then the coefficients at level m will be approximately $1/27$ as large as the analogous coefficients at level $m-1$. Hence at higher levels many coefficients should be small and can be removed in the thresholding step.

8 Numerical examples

To demonstrate the performance of the compression algorithm, we performed experiments with several test functions. In all cases we choose Δ^0 as the triangulation that is constructed by dividing the unit square $[0,1] \times [0,1]$ by its bissectrice in two triangles. We selected six bivariate test functions which are given by

$$\begin{aligned}
f_1(x,y) &= 0.75 \exp\left[-\frac{(9x-2)^2+(9y-2)^2}{4}\right] + 0.75 \exp\left[-\frac{(9x+1)^2}{49} - \frac{(9y+1)}{10}\right] \\
&\quad +0.5 \exp\left[-\frac{(9x-7)^2+(9y-3)^2}{4}\right] - 0.2 \exp\left[-(9x-4)^2-(9y-7)^2\right], \\
f_2(x,y) &= \left(\tanh(9-9x-9y)+1\right)/9, \\
f_3(x,y) &= \left(1.25+\cos(5.4y)\right) / \left(6+6(3x-1)^2\right), \\
f_4(x,y) &= \exp\left[-\frac{81}{4}\left((x-0.5)^2+(y-0.5)^2\right)\right]/3, \\
f_5(x,y) &= \sqrt{64-81\left((x-0.5)^2+(y-0.5)^2\right)}/9 - 0.5, \\
f_6(x,y) &= \begin{cases} \exp\left[-\frac{r_0^2}{r_0^2-r^2}\right], & r < r_0, \\ 0, & \text{otherwise}, \end{cases} \\
&\quad \text{with } r := r(x,y) = (x-0.5)^2+(y-0.5)^2 \text{ and } r_0 = 1/128.
\end{aligned}$$

For each test function f we measure the root mean square (RMS) error between f and s. That is,

$$RMS = \sqrt{\frac{\sum_{i=0}^{M}\sum_{j=0}^{N}\left(f(x_i,y_j)-s(x_i,y_j)\right)^2}{(M+1)(N+1)}},$$

where $x_i = i/M, y_j = j/N$, and $M = N = 100$. We also measure the maximum distance (MD) between f and s,

$$MD = \max_{i=0,\ldots,M, j=0,\ldots,N} |f(x_i,y_j) - s(x_i,y_j)|.$$

To normalize the error values, we divide the RMS error and MD error by the difference of the maximum and minimum values of f over the domain. These normalized error values are denoted by NRMS and NMD. Each test function f_i is approximated by a spline s_l corresponding to level $l = 1$ or $l = 2$, and by a spline s_4 which is compressed with threshold ϵ. We choose the threshold ϵ such that the spline s_4 after compression with threshold ϵ has less non–zero coefficients than the spline s_l. The results are shown in Table 2 and Table 3. The surfaces corresponding to the functions f_i are plotted in Figure 6, the surfaces corresponding to the splines s_l are plotted in Figure 7 and the surfaces corresponding to the compressed splines s_4 are plotted in Figure 8.

9 Application: image compression

Our surface compression algorithm is well suited to any application that can be cast as a surface fitting problem. We can interpret a grayscale image as a surface, where the value of each pixel represents its height. Image compression is then cast into a surface compression framework that can be solved with the algorithm presented in this paper. Derivative information of the image surface can be estimated by applying the Sobel operator [8] to the image.

	f_1	f_2	f_3	f_4	f_5	f_6
l	1	1	2	1	1	2
# coeff	48	48	300	48	48	300
RMS	0.040139	0.012541	0.000158	0.020974	0.001675	0.034707
MD	0.139814	0.035804	0.000989	0.103371	0.007246	0.353521
NRMS	0.032954	0.056434	0.000432	0.062926	0.004783	0.094343
NMD	0.114785	0.161119	0.002698	0.310126	0.020687	0.960970

Table 2: Errors between the test functions $f_i(x, y)$ and the approximating spline $s_l(x, y)$ without compression.

	f_1	f_2	f_3	f_4	f_5	f_6
ϵ	0.1	0.04	0.0008	0.02	0.015	0.01
# coeff	47	45	256	36	48	276
rate	429 to 1	448 to 1	79 to 1	560 to 1	420 to 1	73 to 1
RMS	0.030971	0.009209	0.000159	0.004838	0.001675	0.000772
MD	0.108095	0.024047	0.000647	0.013934	0.007246	0.019024
NRMS	0.025427	0.041442	0.000435	0.014514	0.004783	0.002098
NMD	0.088745	0.108213	0.001765	0.041804	0.020687	0.051713

Table 3: Errors between the test functions $f_i(x, y)$ and the approximating spline $s_4(x, y)$ after compression with threshold ϵ.

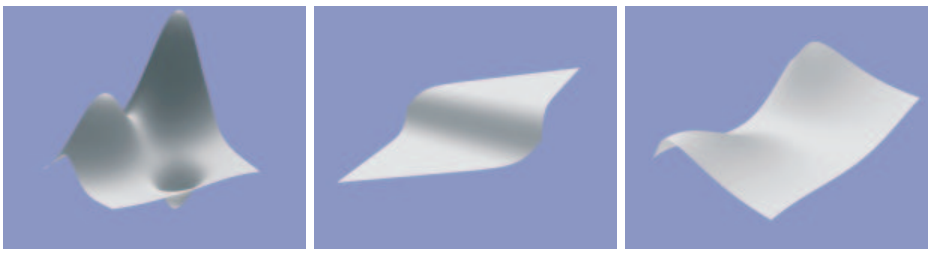

(a) f_1 (b) f_2 (c) f_3



(d) f_4 (e) f_5 (f) f_6

Figure 6: The test functions.

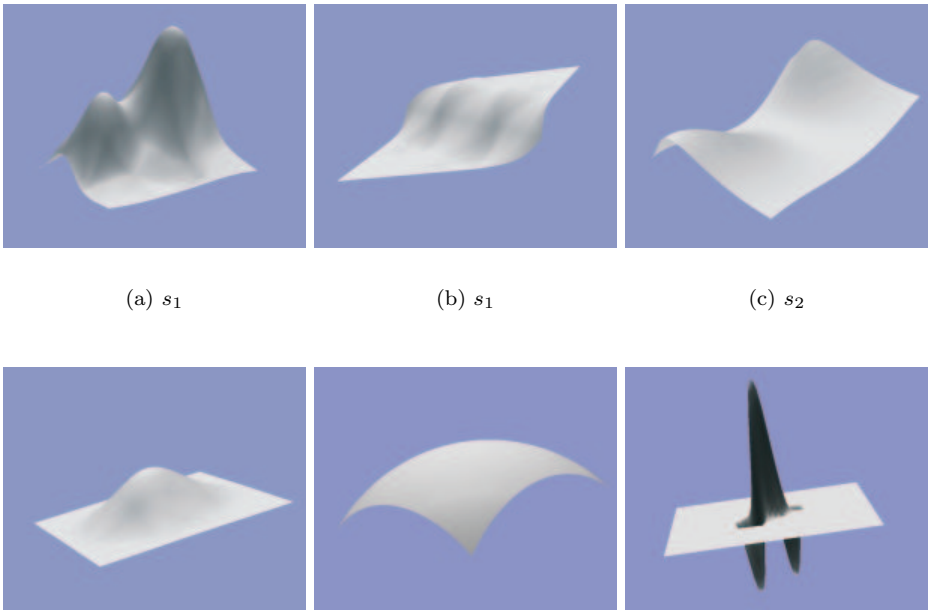

(a) s_1 (b) s_1 (c) s_2

(d) s_1 (e) s_1 (f) s_2

Figure 7: The approximating splines s_l at level $l = 1$ or $l = 2$.

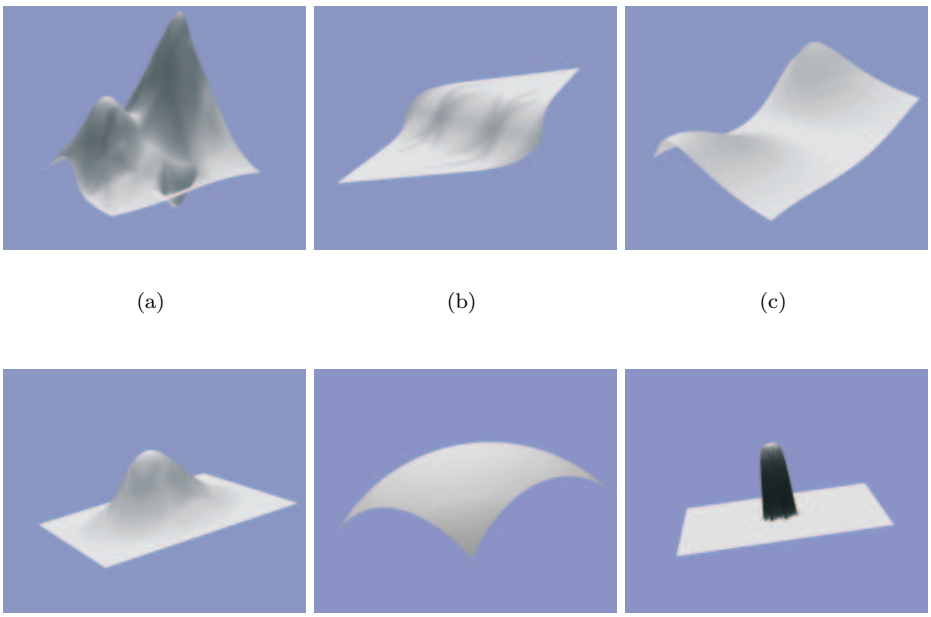

(a) (b) (c)

(d) (e) (f)

Figure 8: The splines s_4 after compression.

The dimensions of the original image in Figure 9a are 512×512. We used a spline s_5 to approximate the original surface. The base domain Δ^0 is constructed by dividing the unit square $[0,1] \times [0,1]$ by its bissectrice in two triangles. The compression algorithm was applied with threshold values ϵ equal to 0.01, 0.02, 0.03, 0.04, and 0.05. The number of non–zero coefficients for the images in Figures 9b - 9f are respectively 79685, 45210, 31237, 22315, 17439. The corresponding compression rates are respectively 3.3 to 1, 5.8 to 1, 8.4 to 1, 11.7 to 1, and 15.0 to 1.

Acknowledgements

This work is partially supported by the Flemish Fund for Scientific Research (FWO Vlaanderen) project MISS (G.0211.02), and by the Belgian Programme on Interuniversity Attraction Poles, initiated by the Belgian Federal Science Policy Office. The scientific responsibility rests with the authors.

References

[1] R. A. Adams. *Sobolev spaces*. Academic Press, New York, 1975.

[2] J. H. Bramble and S. R. Hilbert. Bounds for a class of linear functionals with applications to hermite interpolation. *Numer. Math.*, 16:362–369, 1971.

[3] P. Dierckx. On calculating normalized Powell–Sabin B-splines. *Comput. Aided Geom. Design*, 15(3):61–78, 1997.

[4] G. Farin. Triangular Bernstein–Bézier patches. *Comput. Aided Geom. Design*, 3(2):83–128, 1986.

[5] D. Hong and L. L. Schumaker. Surface compression using a basis of C^1 cubic bivariate spline spaces. *Journal of Computing*, 2004. To appear.

[6] M. Lai and L. Schumaker. On the approximation power of bivariate splines. *Advances in Comp. Math.*, 9:251–279, 1998.

[7] M. Lai and L. Schumaker. Macro–elements and stable local bases for splines on Powell–Sabin splits. *Math. Comp.*, 72:335–354, 2003.

[8] J. S. Lim. *Two Dimensional Signal and Image Processing*. Prentice-Hall, International editions, 1990.

[9] J. Maes, E. Vanraes, P. Dierckx, and A. Bultheel. On the stability of normalized Powell–Sabin B-splines. *J. Comput. Appl. Math.*, 2004. To appear.

[10] M. J. D. Powell and M. A. Sabin. Piecewise quadratic approximations on triangles. *ACM Transactions on Mathematical Software*, 3:316–325, 1977.

[11] E. Vanraes, J. Maes, and A. Bultheel. Powell–Sabin spline wavelets. *Intl. Journal of Wavelets, Multiresolution and Information Processing*, 2(1):23–42, 2004.

[12] E. Vanraes, J. Windmolders, A. Bultheel, and P. Dierckx. Automatic construction of control triangles for subdivided Powell–Sabin splines. *Computer Aided Geometric Design*, 2004. Accepted.



(a) original

(b) 3.3 to 1



(c) 5.8 to 1



(d) 8.4 to 1



(e) 11.7 to 1



(f) 15.0 to 1

Figure 9: Image compression on a picture of Lena.